WARSAW UNIVERSITY OF TECHNOLOGY Index 351733
FACULTY OF CIVIL ENGINEERING
COMMITTEE FOR CIVIL AND WATER ENGINEERING
POLISH ACADEMY OF SCIENCES ISSN 1230-2945

DOI: 10.24425/ace.2026.158602

ARCHIVES OF CIVIL ENGINEERING

Vol. LXXII ISSUE 2 2026

pp. 169 – 182

Research paper

Determination of load-carrying capacity of back-to-back C-profile beams subjected to pure bending

Leszek Czechowski[1], Maria Kotełko[2], Jacek Jankowski[3], Viorel Ungureanu[4], Annabella Sanduly[5], Filip Kaźmierczyk[6]

Abstract: The present work concerns the strength analysis of back-to-back steel C-profiles subjected to pure (4-point) bending. The load-carrying capacities of considered beams were determined using experimental and numerical tests. Numerical analysis was performed using the finite element method (Ansys code) considering the full nonlinearity of the material and large displacement and strains. Three different numerical models were elaborated to adjust the results to experimental ones. The one of numerical models was based on assumption of doubled wall thickness. The experiments have been conducted for beams with two different thicknesses. In the study, the length of the beam and the distance between the supports were taken into account. Two C-beams designated for the tests were connected using spots welds deployed at adequate places. The results of numerical simulations based on different approaches have been compared with those of experimental ones. In general, the results of the numerical simulations are in a good agreement with the experiment.

Keywords: thin-walled structures, experimental tests, load-carrying capacity, pure bending, back-to-back, C-profile, numerical investigations

[1]DSc., Eng., Lodz University of Technology, Faculty of Mechanical Engineering, Stefanowskiego 1/15 St., 90-537 Lodz, Poland, e-mail: leszek.czechowski@p.lodz.pl, ORCID: 0000-0002-4718-6215
[2]Professor, DSc., PhD., Eng., Lodz University of Technology, Faculty of Mechanical Engineering, Stefanowskiego 1/15 St., 90-537 Lodz, Poland, e-mail: maria.kotelko@p.lodz.pl, ORCID: 0000-0001-7784-4349
[3]PhD., Eng., Lodz University of Technology, Faculty of Mechanical Engineering, Stefanowskiego 1/15 St., 90-537 Lodz, Poland, e-mail: jacek.jankowski@p.lodz.pl, ORCID: 0000-0002-9628-2799
[4]Professor, DSc., PhD., Eng., Department of Steel Structures and Structural Mechanics, Politehnica University of Timisoara / Laboratory of Steel Structures, Romanian Academy, Timisoara Branch/Technical Sciences Academy of Romanian (ASTR), 1 Ioan Curea, 300224 Timisoara, Romania, e-mail: viorel.ungureanu@upt.ro, ORCID: 0000-0002-5826-9518
[5]PhD. Student, Lodz University of Technology, Faculty of Mechanical Engineering, Stefanowskiego 1/15 St., 90-537 Lodz, Poland, e-mail: annabella.sanduly@dokt.p.lodz.pl, ORCID: 0000-0003-0568-3181
[6]PhD., Lodz University of Technology, Faculty of Mechanical Engineering, Stefanowskiego 1/15 St., 90-537 Lodz, Poland, e-mail: filip.kazmierczyk@p.lodz.pl, ORCID: 0000-0002-3208-0362

1. Introduction

Back-to-back thin-walled cold-formed steel channel sections (B-BTWCFS) have recently gained increasing application as members in building structures subjected to bending and compression. They usually have stiffened lips on the flanges and/or intermediate stiffeners in the wide flanges and webs. The problem of buckling loads and the load-carrying capacity of single channel section members subjected to simple loading systems (e.g., pure bending, axial compression) can be solved with a good accuracy based on the theory of thin-walled structures and developed in design code specifications such as EN 1993-1-3 [1]. However, the capacity calculation for members of the built-up cross sections is still an open question. In particular, the code recommendations [1] underestimate their load capacity compared to the results of numerical analyses or experimental tests. As observed, most of both the experimental and theoretical work on built-up cross- sections was focused on centric compression of studs either with open sections or closed sections. Based on literature, one can find a few newest papers involving the structural B-BTWCFS behaviour.

Young et al. in [2] presented the comprehensive study on the flexural buckling behaviour of cold-formed steel (CFS) back-to-back built-up columns with Σ-section. They conducted compression tests and numerical simulations to explore the influence of the slenderness ratio and the fastener arrangements. To solve the problem, material characterisation, shearing resistance behaviour of the fastener and imperfection measurements were also considered. They revealed that reducing fastener spacing and increasing shear resistance stiffness improved the load-bearing capacity. The authors of paper [3] focused on slender thin-walled members with fixed ends, which are sensitive to local-global interaction or global buckling. The models were prepared to conduct a parametric study of a compression of members with varying sections, screw arrangements and lengths. These factors were considered to investigate their failures due to local-global interaction and global buckling. They also compared the load- carrying capacities of doubled and individual members and indicated the limitations of the current design equations available in current standards and research publications.

Fang et al. in [4, 5] analysed the compressive behaviour of back- to-back channels with web hole. They presented an experimental and numerical investigation on the behaviour of screw fastened back-to-back built-up aluminium alloy columns. They performed a parametric study to propose equations for the axial strength reduction factor for aluminium alloy back- to-back channels.

Wang et al. [6] analysed the structural performance of back-to-back channels with web holes subjected to axial compression. Roy et al. [7–11] carried out research based on experimental tests and FE modelling of different cross-sections of built-up columns. Dabaon et al. in [12, 13] and Anbarasu et al. in [14, 15] performed experimental tests and numerical simulations of axial compressed cold formed steel (CFS) built-up channels. The authors of the papers [16, 17] explored the buckling behaviour of CFS back- to-back channels. However, Zhang and Young [18–20] analysed the structural performance of built-up CFS channels with stiffeners subjected to axial compression. Young et al. [21, 22] based on the Continuous Strength Method (CSM) investigated the structural behaviour of aluminium alloy channels.

Roy et al. [23–25], Yuan et al. [26] and Dobric et al. [27, 28] performed both experimental and numerical studies of the behaviour of cold-formed stainless steel members with built-up channels cross-sectoion under axial compressive load. Huang and Zhang [29] investigated a high-strength steel welded I-section overall buckling performance with respect to the major axis under combined loads (axial compression and bending). Back-to-back open section beam-columns subjected to eccentric compression (combined compression and bending) were analysed experimentally and numerically by Li and Young [30].

Son Tung Vy et al. [31] presented a very interesting new design approach for back-to-back channel sections of TWCFS under compression. Kotełko et al. [32] showed the results of local plastic failure mechanisms for columns of the lipped channel section subjected to eccentric compression with respect to the minor axis. The continuation of the paper was a work elaborated by Borkowski et al. [33] that relates an experimental programme to the post-failure behaviour of TWCFS members subjected to eccentric compression about the minor axis. Buchanan et al. [34] studied the strength of the circular hollow section beam- columns subjected to eccentric loads. Based on these results, a new approach was established that allowed more realistic predictions of load capacity, contrary to the current EN 1993-1-4 code. Work [35] was devoted to the identification of plastic mechanisms of failure in columns subjected to eccentric compression on both the minor and major axes.

Zhao et al. [36, 37] explored the behaviour of columns with box- type and L-type sections made of aluminium alloy subjected to eccentric load and stainless steel circular hollow sections under combined loads. Zhang et al. in [38] investigated the buckling behaviour of press-braked stainless steel channel section beam-columns under combined compression and under minor-axis bending. A continuation of the work was a study [39], in which theoretically and experimentally press-braked stainless steel channel sections under combined compression were investigated. The investigations mentioned above found that the design methods underestimate the strength in both compressed and eccentrically compressed elements. Back-to-back channel section beams in bending were experimentally tested by Ungureanu et al. [40]. They performed a comprehensive experimental analysis of the buckling resistance of the TWCFS built-up beams.

Based on the newest literature presented above, in the authors' opinion, some recent papers were devoted to the analysis of compression of back-to- back structures, but there is a gap in the research of such structures in bending. This paper presents the investigations of the behaviour of back-to- back C-profile steel members, connected with spot welding, subjected to 4-point bending.

2. Subject and objective of research

The subject of investigation was back-to-back C-profile steel members (DC01) subjected to four-point bending tests (see Fig. 1). The dimensions of columns are the following: l = 1000 mm, a = 150 mm, b = 60 mm, c = 10, t = 1, 1.5 mm.

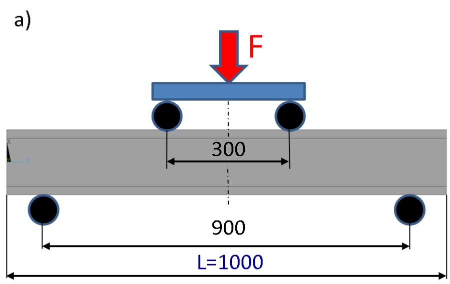

(a)

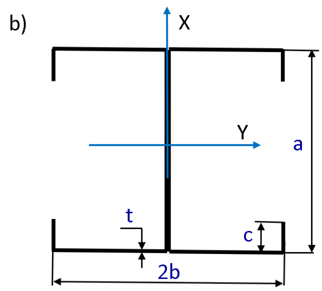

(b)

Fig. 1. Test conditions (a) and dimensions of beam (b)

To avoid local deformations during bending, full solid blocks made of polyamide were partially inserted into empty spaces of analysed beams, as shown in Fig. 2a. In the middle between the load points, the remaining spaces were left empty for observation. The same beam region was also registered by using the ARAMIS® System (DICAS) [41] to accurately notice the deformations of samples that were recorded with frequency 1 Hz. The connections between C-profiles were realised by applying welded spots spaced as was shown in Fig. 2b. The whole tests were conducted until the beams were fully damaged.

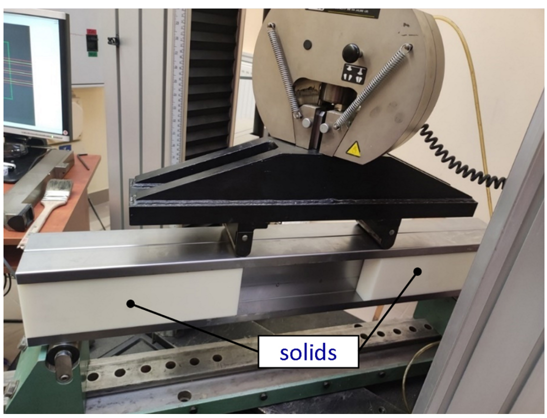

(a)

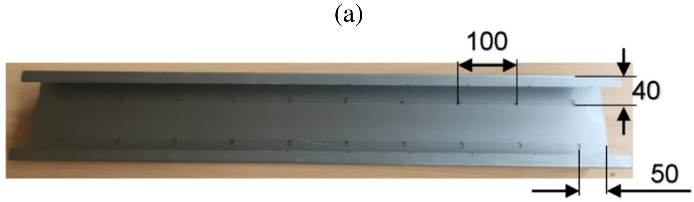

(b)

Fig. 2. Test stand (a) and spacing of spot welds (b)

3. Numerical models

All calculations were performed with Ansys 18.2 software [42]. Tree different numerical models were elaborated to fit the results to experimental ones. The mesh of numerical model was created by applying the 8-node 281-shell element suitable for moderate thin-walled structures and the 20-node 186-solid element. Based on the time consumption for calculation and relative accuracy, the size of the finite element was assumed to be 4 mm. The nonlinear analysis was performed for large strains and the deflections based on Green–Lagrangian equations.

In order to obtain a convergence of numerical calculations for large deformations of the structure, the number of substeps was set from 1000 up to 50,000. In each substep, the maximum number of iterations was allowed to be even 2000. Nonlinear estimations and convergence analysis were performed by means of the Newton-Raphson algorithm. For the purpose of numerical analysis, the perfect structure was taken into account because it was hard to consider some modes of initial imperfection in bending. FE models and the boundary conditions are shown in Figs. 3–5.

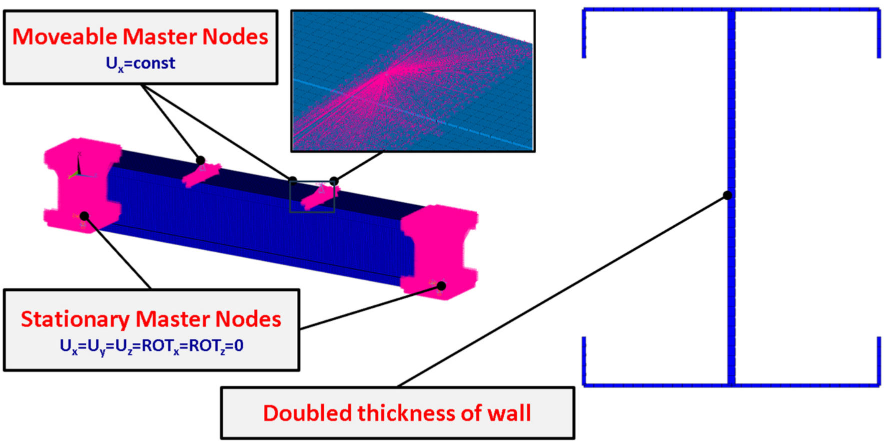

Fig. 3. Numerical model 1 (FEM_1)

The first one, Fig. 3, assumed two webs in contact (I section with lips) with double thickness of the web wall. The load applied to the beam was achieved thanks to two master nodes tied with slave nodes of discrete models. The second one (see Fig. 4) introduced the doubled surfaces between the C-profiles. Moreover, between those neighbouring surfaces, the contact elements were imposed. In addition, small and local connections between touching surfaces were made (by using coupled DOFs in all directions) to model the spot weld connections. The remaining simulation conditions were the same.

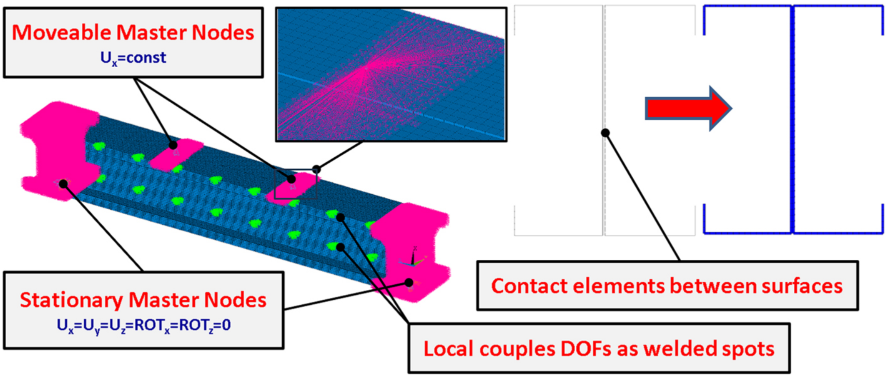

Fig. 4. Numerical model 2 (FEM_2)

The third numerical model (see Fig. 5) was a development of two previous ones in which moveable semicylinders were used to better reflect the real conditions of the tests. Between the cylinders and the beam, contact elements were also used. To reflect the boundary conditions of the conducted experiment, in numerical models, some additional restraints (see Fig. 6) were introduced. It means that some regions (some nodes) of discrete models were linked with each other (dimensions LR1 and LR2). It was necessary to prevent the model from local and accessible deformations that could have lowered the load-carrying capacity of the beams. As mentioned previously, experimental models were partially constrained by inserted solids (solid blocks).

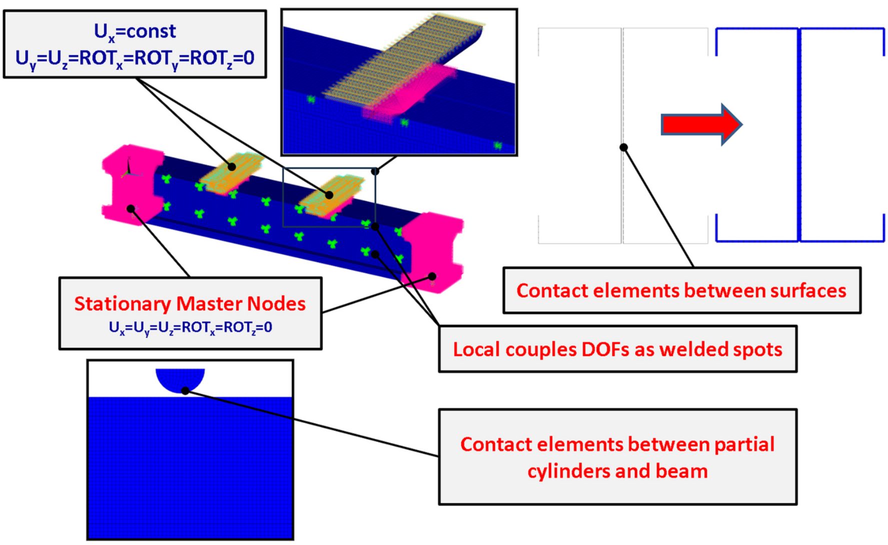

Fig. 5. Numerical model 3 (FEM_3)

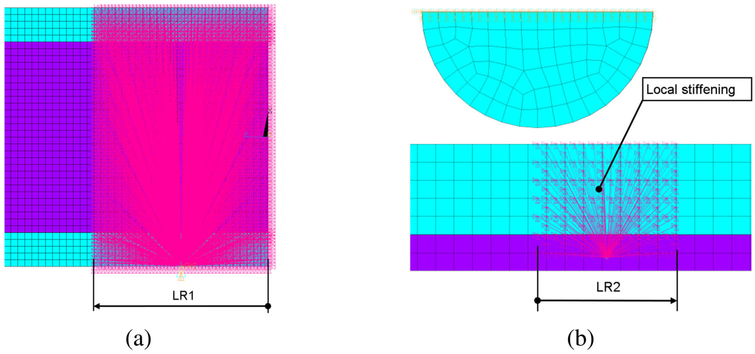

Fig. 6. Extent of stiffening in numerical models a) for FEM_1, FEM_2 and FEM_3 and b) only for FEM_3

The mean one-directional tensile curve (stresses vs. strains) of the material (DC01) based on empirical tests was transformed into the true stress – logarithmic strain (see Fig. 7a – thickness 1 mm and Fig. 7b – thickness 1.5 mm). The average moduli of the analysed materials were 200.8 GPa and 185.9 GPa for 1 mm and 1.5 mm, respectively.

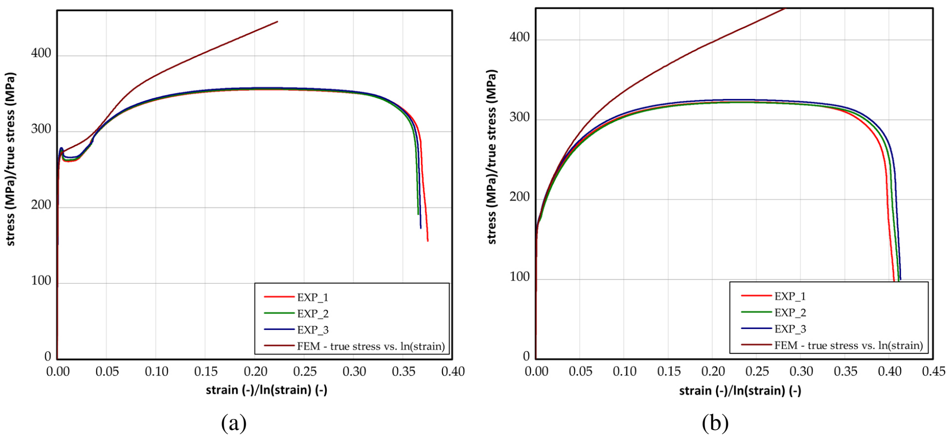

Fig. 7. Curves of one-directional tensile tests in full range for thickness 1 mm (a) and for thickness 1.5 mm (b)

4. Results of analysis

4.1. Equilibrium paths

This section shows the results of the full bending load F versus the deflection of the wall thickness beam, $t = 1$ mm (see Fig. 8) and $t = 1.5$ mm (see Fig. 9). For the first one, the experimental curves are pretty close to each other and the maximum mean load amounted to

30.3 kN (see Table 1). Based on FEM curves, it is easily seen that stiffnesses are greater than in experiment regardless of the case of FEM approaches. The results of FEM_2 for LR1 = 100, 200, 300 mm gave the highest stiffness, but for extent LR1 = 300 mm, the maximum load seemed to be the greatest. The FEM_1 curves (where doubled touching surfaces were assumed) showed slightly lower stiffnesses compared to FEM_2 curves but maximum loads are significantly greater than in the experiment. FEM_3 curves (where semicylinders were used) indicate the best correlation in relation to experimental curves, especially taking into account the maximum loads (see Fig. 8). Of course, one can still see distinct discrepancies, but stiffnesses are smaller. As it turned out, obtaining very close curves in numerical way was not possible, although many attempts at different conditions were conducted. It might be a result of the assumption of perfect model or problems with reflection of accurate boundary conditions. It should be underlined that calculation of each case of FEM_3 took significantly longer than the calculations of FEM_1 and FEM_2. Moreover, preparation of numerical model FEM_3 also required more time and attention; therefore, approaches FEM_1 and FEM_2 can be preliminary used for rough estimations. Taking a look at Fig. 9 (for thickness 1.5 mm), the maximum average load in bending is 49.2 kN (see Table 2). It is 1.6–1.7 times greater than the load for beams of thickness 1 mm. All numerical models showed the greater stiffness relating to experimental curves, but situation repeats as in the previous case, i.e., obtained FEM_3 characteristics (only for LR1 = 100 mm and LR2 = 40 mm or 90 mm) in relation to characteristics of FEM_1 and FEM_2 is of the smallest stiffness.

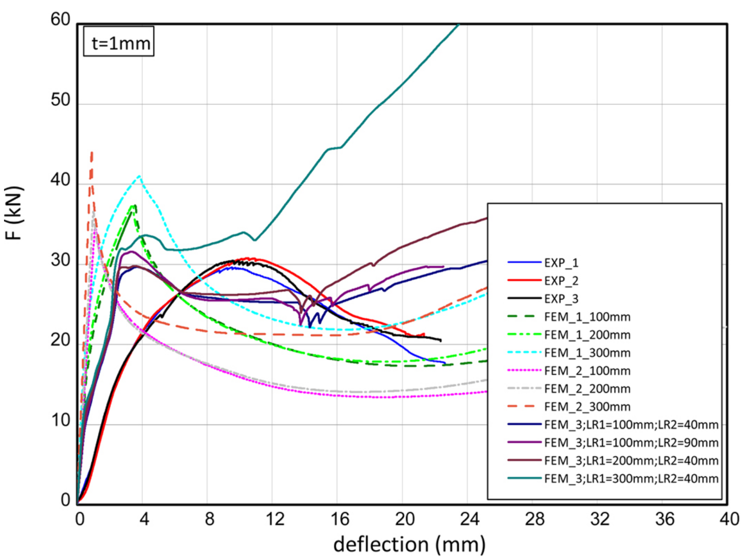

Fig. 8. Load-deflection curves for thickness 1 mm

Of course, they are still far away from the experimental curves, but maximum loads coincide with each other (maximum load was registered about 50 kN). FEM_3 (for LR1 = 200, 300 mm and LR2 = 40 mm) demonstrated the considerable stiffness in contrast to FEM_3 for LR1 = 100 mm (the character of the curves resembles rather a trend of the curves FEM_2). It might be caused due to a change of the zone of deformation. Reinforcements (extent LR1) influence both the stiffness and attained peaks of loads (differences are by a few kN).

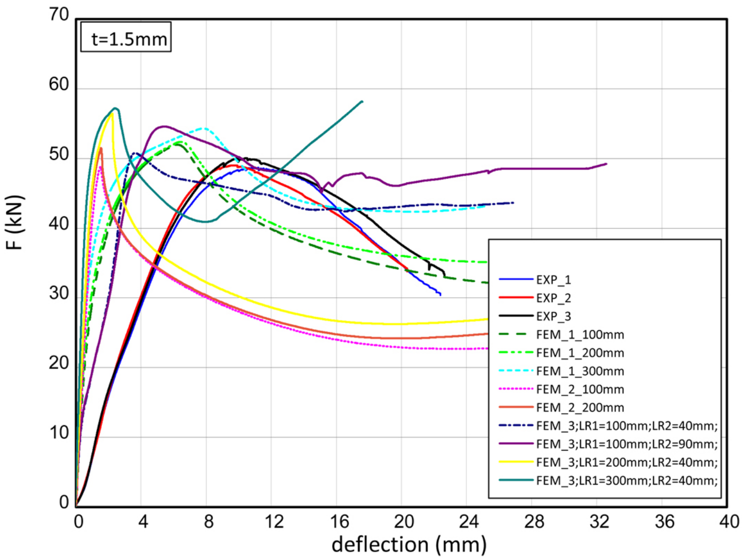

Fig. 9. Load-deflection curves for thickness 1.5 mm

Table 1. Maximum loads for all presented variants for t = 1 mm

LR1(mm)	FEM_1 (kN)	FEM_2 (kN)	FEM_3 (kN)	FEM_avg (kN)
100	34.8	34.1	29.7 (LR2 = 40 mm) 31.6 (LR2 = 90 mm)	30.3
200	37.5	37.1	29.8	
300	41.0	44.2	33.6	

Table 2. Maximum loads for all presented variants for t = 1.5 mm

LR1(mm)	FEM_1 (kN)	FEM_2 (kN)	FEM_3 (kN)	FEM_avg (kN)
100	51.9	48.7	50.8 (LR2 = 40 mm) 54.6 (LR2 = 90 mm)	49.2
200	52.4	51.5	56.5	
300	54.3	n/d	57.2	

4.2. Deformation maps

The deformation maps obtained by DICAS [41] and FE calculations are shown in Figs. 10 and 11. Fig. 10 shows the maps for load peaks and in the early and late post-buckling state (where a significant deflection occurred).

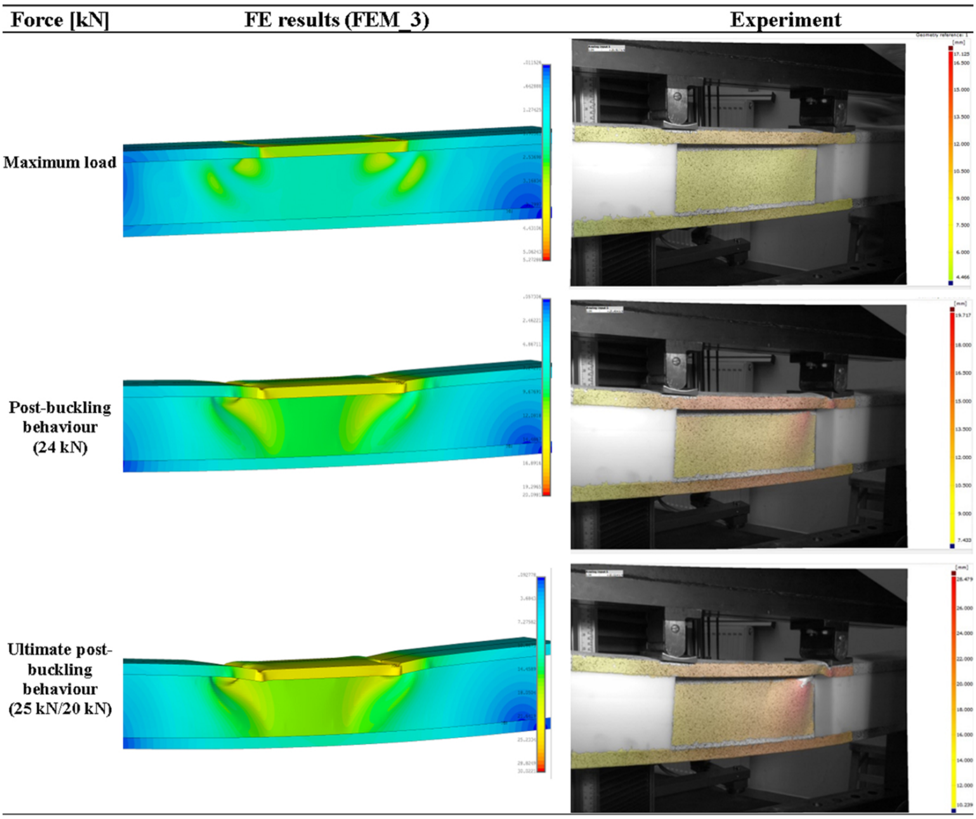

Fig. 10. Maps of deformations achieved by using FEM_3 and DICAS (for 1 mm)

Based on maps results, some correlations could be seen. During the registration of maximum loads, the numerical models showed wrinkles near the points of load application. These details in the sample were not observed in the experiment. With increasing force, local deformations appeared in the experiment on the one side of the sample (the numerical model behaved symmetrically). Based on scales, values of displacements appearing during experiment vs. numerical results are rather comparable (see Figs. 10, 11). The behaviour of the the real samples (both thickness 1 mm and 1.5 mm) was similar. Between the applied points of loads for the ultimate load, distinct buckling modes of the web were recorded.

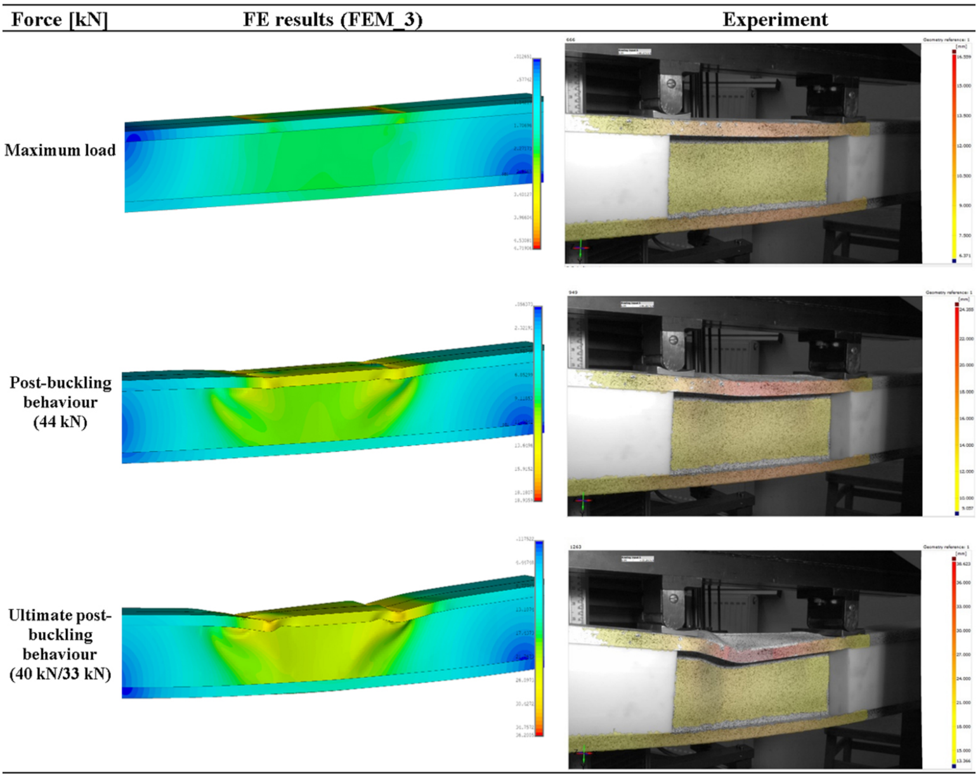

Fig. 11. Maps of deformations achieved by using FEM_3 and DICAS (for 1.5 mm)

5. Conclusions

The paper involves the results of 4-point bending of back-to-back steel C-profiles based on the numerical approach and experimental tests. With respect to the obtained results, some conclusions can be drawn:

i. The mean maximum bending loads were 30.3 kN and 49.2 kN for 1 mm and 1.5 mm, respectively. Repeatability of results for each thickness considered in experiment was satisfactory.
ii. The numerical results compared to the experimental ones showed some similarities. Model FEM_3 among the considered models allowed to get close to experimental curves, but discrepancies in stiffness were also noticed. FEM_1 and FEM_2 gave both the highest maximum loads and stiffnesses. All differences might be the result of assumptions of not entirely adequate boundary conditions in the numerical approach.
iii. Observed beam deformation maps usually indicated the unsymmetrical behaviour in contrast to deformations maps obtained numerically. This effect can be easily explained because during fitting set at the beginning initial and local deformations in samples might have occurred that apparently caused unsymmetrical loading distributions.

Acknowledgments

This work was supported by a grant 2019/35/B/ST8/02823 – Implementation of yield line theory to the load-capacity estimation of thin-walled members under combined load, of the National Science Centre of the Polish Ministry of Science and Higher Education.

The article was co-financed from the state budget of Poland and awarded by the Minister of Science within the framework of the Excellent Science II Programme.

References

[1] EN 1993-1-3 Eurocode 3: Design of Steel Structures, Part 1.3: General Rules, Supplementary Rules for Cold-formed Thin Gauge Members and Sheeting. CEN, Brussels, Belgium, 2006.

[2] J. Yang, K. Luo, W. Wang, Y. Shi, and H. Li, "Research on the flexural buckling behavior of the cold-formed steel back-to-back built-up columns with Σ-section", *Engineering Structures*, vol. 302, art. no. 117404, 2024, doi: 10.1016/j.engstruct.2023.117404.

[3] S.T. Vy and M. Mahendran, "DSM design of fixed-ended slender built-up back- to-back cold-formed steel compression members", *Journal of Constructional Steel Research*, vol. 189, art. no. 107053, 2022, doi: 10.1016/j.jcsr.2021.107053.

[4] Z. Fang, K. Roy, B. Chen, Z. Xie, J. Ingham, and J.B.P. Lim, "Effect of the web hole size on the axial capacity of back-to-back aluminium alloy channel section column", *Engineering Structures*, vol. 260, art. no. 114238, 2022, doi: 10.1016/j.engstruct.2022.114238.

[5] Z. Fang, K. Roy, B. Chen, Z. Xie, and J.B.P. Lim, "Local and distortional buckling behaviour of aluminium alloy back-to-back channels with web holes under axial compression", *Journal of Building Engineering*, vol. 47, art. no. 103837, 2022, doi: 10.1016/j.jobe.2021.103837.

[6] C.G. Wang, Q.L. Guo, Z.G. Zhang, and Y.T. Guo, "Experimental and numerical investigation of perforated cold-formed steel built-up I-section columns with web stiffeners and complex edge stiffeners", *Advances in Structural Engineering*, vol. 22, no. 10, pp. 2205–2221, 2019, doi: 10.1177/1369433219836174.

[7] B. Chen, K. Roy, A. Uzzaman, G. Raftery, and J.B.P. Lim, "Axial strength of back-to-back cold-formed steel channels with edge-stiffened holes, un- stiffened holes and plain webs", *Journal of Constructional Steel Research*, vol. 174, art. no. 106313, 2020, doi: 10.1016/j.jcsr.2020.106313.

[8] K. Roy, T.C.H. Ting, H.H. Lau, and J.B.P. Lim, "Effect of thickness on the behaviour of axially loaded back-to-back cold-formed steel built-up channel sections – Experimental and numerical investigation", *Structures*, vol. 16, pp. 327–346, 2018, doi: 10.1016/j.istruc.2018.09.009.

[9] T.C.H. Ting, K. Roy, H.H. Lau, and J.B.P. Lim, "Effect of screw spacing on behavior of axially loaded back-to-back cold-formed steel built-up channel sections", *Advances in Structural Engineering*, vol. 21, no. 3, pp. 474–487, 2018, doi: 10.1177/1369433217719986.

[10] K. Roy, T.C.H. Ting, H.H. Lau, and J.B.P. Lim, "Nonlinear behavior of back- to-back gapped built-up cold-formed steel channel sections under compression", *Journal of Constructional Steel Research*, vol. 147, pp. 257–276, 2018, doi: 10.1016/j.jcsr.2018.04.007.

[11] K. Roy, H.H. Lau, and J.B.P. Lim, "Numerical investigations on the axial strength of back-to-back gapped built-up cold-formed stainless steel channels", *Advances in Structural Engineering,* vol. 22, no. 10, pp. 2289–2310, 2019, doi: 10.1177/1369433219837390.

[12] M. Dabaon, E. Ellobody, and K. Ramzy, "Experimental investigation of built- up cold-formed steel section battened columns", *Thin-Walled Structures*, vol. 92, pp. 137–145, 2015, doi: 10.1016/j.tws.2015.03.001.

[13] M. Dabaon, E. Ellobody, and K. Ramzy, "Nonlinear behaviour of built-up cold- formed steel section battened columns", *Journal of Constructional Steel Research*, vol. 110, pp. 16–28, 2015, doi: 10.1016/j.jcsr.2015.03.007.

[14] M. Anbarasu, K. Kanagarasu, and S. Sukumar, "Investigation on the behaviour and strength of cold-formed steel web stiffened built-up battened columns", *Materials and Structures*, vol. 48, no. 12, pp. 4029–4038, 2014, doi: 10.1617/s11527-014-0463-8.

[15] M. Anbarasu, "Behaviour of cold-formed steel built-up battened columns composed of four lipped angles: tests and numerical validation", *Advances in Structural Engineering*, vol. 23, no. 1, pp. 51–64, 2019, doi: 10.1177/1369433219865696.

[16] D.C. Fratamico, S. Torabian, X. Zhao, K.J.R. Rasmussen, and B.W. Schafer, "Experiments on the global buckling and collapse of built-up cold-formed steel columns", *Journal of Constructional Steel Research,* vol. 144, pp. 65–80, 2018, doi: 10.1016/j.jcsr.2018.01.007.

[17] D.C. Fratamico, S. Torabian, X. Zhao, K.J.R. Rasmussen, and B.W. Schafer, "Experimental study on the composite action in sheathed and bare built-up cold-formed steel columns", *Thin-Walled Structures*, vol. 127, pp. 290–305, 2018, doi: 10.1016/j.tws.2018.02.002.

[18] J.H. Zhang and B. Young, "Finite element analysis and design of cold-formed steel built-up closed section columns with web stiffeners", *Thin- Walled Structures*, vol. 131, pp. 223–237, 2018, doi: 10.1016/j.tws.2018.06.008.

[19] J.H. Zhang and B. Young, "Numerical investigation and design of cold-formed steel built-up open section columns with longitudinal stiffeners", *Thin-Walled Structures*, vol. 89, pp. 178–191, 2015, doi: 10.1016/j.tws.2014.12.011.

[20] J.H. Zhang and B. Young, "Compression tests of cold-formed steel built-up open sections with edge and web stiffeners", *Thin-Walled Structures*, vol. 52, pp. 1–11, 2012, doi: 10.1016/j.tws.2011.11.006.

[21] M.N. Su, B. Young, and L. Gardner, "Continuous strength method for aluminium alloy structures", *Advanced Materials Research*, vol. 742, pp. 70–75, 2013, doi: 10.4028/www.scientific.net/AMR.742.70.

[22] M.N. Su, B. Young, and L. Gardner, "Testing and design of aluminium alloy cross sections in compression", *Journal of Structural Engineering*, vol. 140, no. 9, art. no. 04014047, 2014, doi: 10.1061/(ASCE)ST.1943-541X.0000972.

[23] K. Roy, H.H. Lau, and J.B.P. Lim, "Finite element modelling of back-to-back built-up cold-formed stainless-steel lipped channels under axial compression", *Steel and Composite Structures*, vol. 33, pp. 37–66, 2019, doi: 10.12989/scs.2019.33.1.037.

[24] K. Roy and J.B.P. Lim, "Numerical investigation into the buckling behaviour of face-to-face built-up cold-formed stainless steel channel sections under axial compression", *Structures*, vol. 20, pp. 42–73, 2019, doi: 10.1016/j.istruc.2019.02.019.

[25] K. Roy, H.H. Lau, and J.B.P. Lim, "Numerical investigations on the axial capacity of back-to-back gapped built-up cold-formed stainless steel channels", *Advances in Structural Engineering*, vol. 22, no. 10, pp. 2289–2310, 2019, doi: 10.1177/1369433219837390.

[26] H.X. Yuan, Y.Q. Wang, Y.J. Shi, and L. Gardner, "Stub column tests on stainless steel built-up sections", *Thin-Walled Structures*, vol. 83, pp. 103–114, 2014, doi: 10.1016/j.tws.2014.01.007.

[27] J. Dobrić, Z. Marković, D. Budevac, M. Spremić, and N. Fric, "Resistance of cold-formed built-up stainless steel columns – Part I: Experiment", *Journal of Constructional Steel Research*, vol. 145, pp. 552–572, 2018, doi: 10.1016/j.jcsr.2018.02.026.

[28] J. Dobrić, M. Pavlović, Z. Marković, D. Budevac, and M. Spremić, "Resistance of cold-formed built-up stainless steel columns – Part II: numerical simulation", *Journal of Constructional Steel Research*, vol. 140, pp. 247–260, 2018, doi: 10.1016/j.jcsr.2017.10.032.

[29] B. Huang and W.F. Zhang, "Overall buckling performance of high strength steel welded I-sections under combined axial compression and bending", *Archives of Civil Engineering*, vol. 68, no. 3, pp. 369–384, 2022, doi: 10.24425/ace.2022.141891.

[30] Q.-Y. Li and B. Young, "Design of cold-formed steel built-up open section members under combined compression and bending", *Thin-Walled Structures*, vol. 172, art. no. 108890, 2022, doi: 10.1016/j.tws.2022.108890.

[31] S.T. Vy, M. Mahendran, et al., "A consistent design approach for built-up back-to-back CFS channel compression members with varying boundary conditions and sheathing effects", in *Proceedings of 9th Int. Conference on Thin-Walled Structures – ICTWS 2023*. Sydney, Australia, 420, 2023.

[32] M. Kotełko, J. Grudziecki, V. Ungureanu, and D. Dubina, "Ultimate and post- ultimate behaviour of thin-walled cold-formed steel open-section members under eccentric compression. Part I: Collapse mechanisms database (theoretical study)", *Thin-Walled Structures*, vol. 169, art. no. 108366, 2021, doi: 10.1016/j.tws.2021.108366.

[33] Ł. Borkowski, J. Grudziecki, M. Kotełko, V. Ungureanu, and D. Dubina, "Ultimate and post-ultimate behaviour of thin-walled cold-formed steel open- section members under eccentric compression. Part II: Experimental study", *Thin-Walled Structures*, vol. 171, art. no. 108802, 2022, doi: 10.1016/j.tws.2021.108802.

[34] C. Buchanan, O. Zhao, E. Real, and L. Gardner, "Cold-formed stainless steel CHS beam-columns – Testing, simulation and design", *Engineering Structures*, vol. 213, art. no. 110270, 2020, doi: 10.1016/j.engstruct.2020.110270.

[35] V. Ungureanu, I. Both, M. Kotełko, L. Czechowski, F. Bodea, and D. Dubina, "Buckling strength and post-ultimate behaviour of lipped channel section short columns under eccentric compression", *Thin-Walled Structures*, vol. 181, art. no. 110085, 2022, doi: 10.1016/j.tws.2022.110085.

[36] O. Zhao, L. Gardner, and B. Young, "Structural performance of stainless steel circular hollow sections under combined axial load and bending – Part 1: Experiments and numerical modeling", *Thin-Walled Structures*, vol. 101, pp. 231–239, 2016, doi: 10.1016/j.tws.2015.12.003.

[37] Y. Zhao, X. Zhai, and L. Sun, "Test and design method for the buckling behaviors of 6082-T6 aluminum alloy columns with box-type and L-type sections under eccentric compression", *Thin-Walled Structures*, vol. 100, pp. 62–80, 2016, doi: 10.1016/j.tws.2015.12.010.

[38] L. Zhang, S. Li, K.H. Tan, and O. Zhao, "Experimental and numerical investigations of press-braked stainless steel channel section beam- columns", *Thin-Walled Structures*, vol. 161, art. no. 107344, 2021, doi: 10.1016/j.tws.2020.107344.

[39] L. Zhang, Y. Zhong, and O. Zhao, "Press-braked stainless steel channel sections under major axis combined loading: tests, simulations and design", *Journal of Constructional Steel Research,* vol. 187, art. no. 106932, 2021, doi: 10.1016/j.jcsr.2021.106932.

[40] V. Ungureanu, I. Both, F. Bodea, and I. Lukacević, "Experimental study on the buckling resistance of cold-formed steel back-to-back plain and lipped channels in bending", in *Proceedings of the Cold-Formed Steel Research Consortium Colloquium, 17–19 October, 2022*.

[41] Z.L. Kahn-Jetter and T.C. Chu, "Three-dimensional displacement measurements using digital image correlation and photogrammic analysis", *Experimental Mechanics*, vol. 30, no. 1, pp. 10–16, 1990, doi: 10.1007/BF02322695.

[42] Ansys, *User's Guide,* 18.2, Inc.: Houston, TX, USA, 2018.

Wyznaczenie nośności złożonych profili ceowych poddanych czystemu zginaniu

Słowa kluczowe: konstrukcje cienkościenne, nośność graniczna przy zginaniu, podwójny profil ceowy

Streszczenie:

Praca dotyczy wyznaczania numerycznie i eksperymentalnie nośności zimno formowanych stalowych belek otwartych o grubościach 1 mm i 1,5 mm z żebrami na pasach typu „back-to-back" przy zginaniu czteropunktowym. Belki były łączone ze sobą za pomocą punktowych spoin. Symulacje zginania belek zostały przeprowadzone stosując metodę elementów skończonych (program Ansys) z uwzględnieniem pełnych charakterystyk materiałowych w układnie logarytmicznym oraz nieliniowości geometrycznych. Do walidacji modelu numerycznego zastosowano trzy różne modele numeryczne. Wybrane wyniki symulacji zostały porównane z wynikami uzyskanymi empirycznie. Deformacje belek w trakcie wykonywania badań doświadczalnych były rejestrowane optyczną metodą cyfrowej korelacji obrazów za pomocą systemu Aramis w celu określenia map deformacji i wielkości przemieszczeń punktów dla określonego obciążenia. Wyniki analizy pokazały, iż wyniki symulacji numerycznych pod względem nośności dały porównywalne wyniki względem doświadczalnych, natomiast wykazały większą sztywność.

Received: 2025-02-26, Revised: 2025-04-23